

Strontium ranelate promotes increased peri-implant bone formation in ovariectomized rats

Ranelato de Estrôncio promove aumento na formação óssea peri-implantar em ratas ovariectomizadas

El ranelato de estroncio promueve el aumento de la formación ósea periimplantaria en ratas ovariectomizadas

Received: 10/06/2020 | Reviewed: 10/14/2020 | Accept: 10/15/2020 | Published: 10/18/2020

Fernanda Costa Yogui

ORCID: <https://orcid.org/0000-0002-0760-7337>

Universidade Estadual Paulista "Júlio de Mesquita Filho", Brazil

E-mail: fernanda.yogui@gmail.com

Ana Cláudia Ervolino-Silva

ORCID: <https://orcid.org/0000-0002-6592-0460>

Universidade Estadual Paulista "Júlio de Mesquita Filho", Brazil

E-mail: anaervolino@hotmail.com

Letícia Pitol-Palin

ORCID: <https://orcid.org/0000-0003-4765-3765>

Universidade Estadual Paulista "Júlio de Mesquita Filho", Brazil

E-mail: leticiappalin@gmail.com

Juliana Zorzi Coléte

ORCID: <https://orcid.org/0000-0001-9957-2073>

Universidade Estadual Paulista "Júlio de Mesquita Filho", Brazil

E-mail: juliana.zorzi@uenp.edu.br

Jaqueline Suemi Hassumi

ORCID: <https://orcid.org/0000-0002-5214-1214>

Universidade Estadual Paulista "Júlio de Mesquita Filho", Brazil

E-mail: jaquelinehassumi@hotmail.com

Naara Gabriela Monteiro

ORCID: <https://orcid.org/0000-0002-2857-9195>

Universidade Estadual Paulista "Júlio de Mesquita Filho", Brazil

E-mail: naaragmonteiro@gmail.com

Fábio Roberto de Souza Batista

ORCID: <https://orcid.org/0000-0002-5105-7686>

Universidade Estadual Paulista "Júlio de Mesquita Filho", Brazil

E-mail: fabiorsbatista@gmail.com

Pedro Henrique Silva Gomes-Ferreira

ORCID: <https://orcid.org/0000-0002-8936-3662>

Universidade Estadual Paulista "Júlio de Mesquita Filho", Brazil

E-mail: pedroferreirabmf@gmail.com

Roberta Okamoto

ORCID: <https://orcid.org/0000-0002-6773-6966>

Universidade Estadual Paulista "Júlio de Mesquita Filho", Brazil

E-mail: roberta.okamoto@unesp.br

Abstract

This study aimed to evaluate the systemic effect of strontium ranelate (SR) on peri-implant bone tissue. Thirty-six adult rats were divided into three experimental groups: sham (SHAM), ovariectomized (OVX) and ovariectomized rats treated with strontium ranelate (OVX-Sr). Strontium ranelate (625mg/kg) was administered by oral gavage on a daily basis. The implants were installed on the tibiae. The euthanasia occurred 42 and 60 days after the implants were installed, and the biomechanical (reverse torque); PCR-RT; histological; immunohistochemical; confocal microscopy and histometric analysis were performed. Quantitative data was subjected to statistical tests with significance level set at $p < 0.05$. Significant increase in implant reverse torque in OVX-Sr was observed when compared to OVX. PCR analysis showed an increase in the genetic expression of the proteins responsible for bone formation in OVX-SR. In the histological analysis, SHAM and OVX-Sr showed a higher degree of maturation of peri-implant bone tissue. Ran-Sr presented higher immunolabeling for ALP and OPN proteins when compared to OVX. In the confocal microscopy, OVX-Sr there was good bone neof ormation showed by incorporation of Alizarin red fluorochrome. The histometric analysis, bone implant contact (BIC) and neof ormed bone area (NBA) presented statistically difference among all groups, and the Ran-Sr presented the highest BIC. Thus, strontium ranelate improves osseointegration and quality of neof ormed bone tissue around implants in estrogen deficient rats.

Keywords: Osteoporosis; Strontium; Osseointegration; Bone.

Resumo

Este estudo objetiva avaliar o efeito sistêmico do ranelato de estrôncio (SR) no tecido ósseo peri-implantar. Trinta e seis ratas adultas foram divididas em três grupos experimentais: SHAM (SHAM), ovariectomizadas (OVX) e ovariectomizadas tratadas com ranelato de estrôncio (OVX-Sr). O ranelato de estrôncio (625mg/kg) era administrado por gavagem oral diariamente. Os implantes foram instalados na tíbia. A eutanásia ocorreu 42 e 60 dias após a instalação dos implantes, e a biomecânica (torque reverso); PCR-RT; histológica; imunohistoquímica; microscopia confocal e análise histométrica foram realizadas. Os dados quantitativos foram submetidos a testes estatísticos com nível de significância fixado em $p < 0,05$. Foi observado um aumento significativo do torque reverso do implante em OVX-Sr quando comparado com OVX. A análise por PCR mostrou um aumento na expressão genética das proteínas responsáveis pela formação óssea em OVX-SR. Na análise histológica, SHAM e OVX-Sr mostraram um maior grau de maturação do tecido ósseo peri-implantar. OVX-Sr apresentou uma maior imunomarcagem para as proteínas ALP e OPN quando comparadas com as OVX. Na microscopia confocal, OVX-Sr houve boa neoformação óssea mostrada pela incorporação de fluorocromo vermelho de Alizarina. A análise histométrica, o contacto do implante ósseo (BIC) e a área óssea neoformada (NBA) apresentaram diferenças estatísticas entre todos os grupos, e o Ran-Sr apresentou o BIC mais elevado. Assim, o ranelato de estrôncio melhora a osseointegração e a qualidade do tecido ósseo neoformado em torno de implantes em ratos deficientes em estrogênio.

Palavras-chave: Osteoporose; Estrôncio; Osseointegração; Osso.

Resumen

Este estudio tiene como objetivo evaluar el efecto sistémico del ranelato de estroncio (SR) en el tejido óseo periimplantario. Treinta y seis ratas adultas fueron divididas en tres grupos experimentales: SHAM (SHAM), ovariectomizadas (OVX) y ovariectomizadas tratadas con ranelato de estroncio (OVX-Sr). El ranelato de estroncio (625mg/kg) se administró por vía oral diariamente. Los implantes se instalaron en la tibia. La eutanasia se produjo 42 y 60 días después de la instalación del implante, y se realizaron análisis biomecánicos (torsión inversa); PCR-RT; histológicos; inmunohistoquímicos; microscopía confocal e histométricos. Los datos cuantitativos se sometieron a pruebas estadísticas con un nivel de significación establecido en $p < 0,05$. Se observó un aumento significativo del torque inverso del implante en OVX-Sr en comparación con OVX. El análisis por PCR mostró un aumento en la expresión genética de las proteínas responsables de la formación de huesos en OVX-SR. En el análisis

histológico, SHAM y OVX-Sr mostraron un mayor grado de maduración del tejido óseo periimplantario. OVX-Sr mostró una marca de inmunidad más alta para las proteínas ALP y OPN en comparación con OVX. En la microscopía confocal, OVX-Sr hubo una buena neoformación ósea mostrada por la incorporación del fluorocromo rojo de Alizarin. El análisis histórico, el contacto con el implante óseo (BIC) y el área ósea neoformada (NBA) mostraron diferencias estadísticas entre todos los grupos, y Ran-Sr mostró el BIC más alto. Así, el ranelato de estroncio mejora la osteointegración y la calidad del tejido óseo neoformado alrededor de los implantes en ratas con deficiencia de estrógeno.

Palabras clave: Osteoporosis; Estroncio; Oseointegración; Hueso.

1. Introduction

Osteoporosis is the principal systemic skeletal disease characterized by decreased bone density and a deterioration in bone quality (Compston et al. 2019; Cosman et al. 2014), can be classified primarily as juvenile, postmenopausal, and senile osteoporosis and secondarily is related to several diseases, such as endocrine, hematological, rheumatic, gastrointestinal, or from medications such as glucocorticoids (Tarantino et al. 2017). This disease mainly affects as postmenopausal women, is estimated to affect 200 million women worldwide approximately (International Osteoporosis Foundation), in addition, fractures resulting from osteoporosis are a major cause of morbidity and mortality in the elderly (Compston et al. 2019).

Many elderly patients are looking for a rehabilitative treatment with dental implants and they may be taking or have taken any osteoporosis drug. There are several medications for treating osteoporosis. Among them, we have the antiresorptives such as bisphosphonates, denosumab and selective estrogen receptor modulators (SERMs), the proformative agent teriparatide and the antiresorptive/ proformative compound strontium ranelate (Tarantino et al. 2017).

Strontium ranelate is composed of two atoms of stable strontium and an organic portion of ranelic acid. This drug acts by the activation of the calcium-sensitive receptor and leads to OPG increase as well as RANKL decrease (Hamdy, 2009; Hurtel-Lemaire et al, 2009), showing a double action mechanism, stimulating bone neoformation and suppressing bone resorption (Pilmane et al. 2017; Bonnelye et al. 2008). Besides the good action in bone tissue (Grynepas at al. 1990), with reduction on vertebral and non-vertebral fracture in postmenopausal women (Meunier et al. 2004; Reginster et al. 2005), RE is strongly related to skin

adverse effects (Confavreux et al. 2012) and cardiovascular changes as well as myocardium heart attack. Therefore, RE indication is restricted to patients with severe osteoporosis when other available treatments are not enough to fight to this disease (Reginster et al 2015). It is also contraindicated in ischemical diseases in heart, periferical arterial disease (EMA).

Often ovariectomized female rats are used to simulate postmenopausal women, because of estrogen deficiency caused by ovariectomy and consequently decreased bone quality (Beattie JR et al. 2019). Similarly, Implant placement in tibial metaphysis is widely used to assess osseointegration (Glösel et al 2010; Yogui et al 2018; Palin et al 2018; Ramalho-Ferreira et al 2015). Thus, the aim of this study was to evaluate the systemic effect of strontium ranelate (SR) on peri-implant bone tissue, having as null hypothesis that strontium ranelate treatment does not influence osseointegration.

2. Methodology

2.1 Animals

Rats was used as animal model for osteopenia and implants installed in rat tibias is a widely used model for evaluating osseointegration (Faverani et al. 2018; Lii et al. 2012). This research was approved by the Ethics Committee on the Use of Animals of Dental School of the Univ. Estadual Paulista - UNESP (CEUA - Protocol N°. 2015-00616). Thirty-six female Wistar rats (*Rattus novergicus albinus*), 6 months old, and 300g body weight were used. The animals were divided randomly into three experimental groups: control rats (SHAM), estrogen deficient rats (OVX) and estrogen deficient rats and medicated with strontium ranelate (OVX-SR). The animals were fed with rations for laboratory animals (Presence, Neovia nutrition and animal health LTDA, Paulínea, SP, Brazil) and water ad libitum, in a room maintained at 20°C with a 12-hr/12-hr light/dark cycle. All measures were taken to minimize the number of animals used and to avoid suffering. Experimental manipulation procedures were performed according to the norms established by the ARRIVE Guidelines (Kilkenny et al. 2010).

2.2 Osteopenia induction and drug treatment

The 36 rats were anesthetized with 50mg/kg intramuscular ketamine hydrochloride 10% (Dopalen, Ceva Animal Health Ltda, Paulínea, SP, Brazil) and 5mg/kg of xylazine hydrochloride 2% (Anasedan, Ceva Animal Health Ltda, Paulínea, SP, Brazil), and then

performed incisions on both flanks, with ovarian exposure and surgical removal. The suture was made by planes with absorbable suture thread (Poligalactin 910, Vycril 4.0, Ethicon Endo-surgery, São Paulo, SP, Brazil). For the SHAM, 12 rats were submitted only to the ovaries exposition, without their removal, with the intention of subjecting the rats to the same surgical stress, as the ovariectomized ones.

After 30 days of ovariectomy, was started the treatment with strontium ranelate (Protos, Servier laboratory, Gidy, França) in Ran-Sr rats. The drug was administered by gavage using a gavage needle for rats at the daily dose of 625mg/kg/day (Bain et al. 2009; Maimoun et al. 2010; Zacchetti et al. 2014), dissolved in aqueous solution, until the end of the experiment.

2.3 Implant placement

30 days after the beginning of the drug treatment, the animals were submitted to implant surgery. The rats were anesthetized, with intramuscular ketamine and xylazine hydrochloride and received 0.3ml/kg of mepivacaine hydrochloride with epinephrine (Mepiadre 100, DFL industry and trade, Rio de Janeiro, RJ, Brazil) for local anesthesia and hemostasis.

After sedating the animals, the tricotomy was performed in the medial portion of the right and left tibia and antisepsis of the region was performed with Polyvinyl Pyrrolidone Degermant Iodine (Riodeine Degermante, Rioquímica, São José do Rio Preto, SP, Brazil). An incision of approximately 1.5cm long was made in the left and right tibial metaphysis region using a blade number 15 (Adventive, Basemed Surgical, São Paulo, SP, Brasil), and the soft tissue was divulsed with the aid of periosteal detachers, exposing the bone to receive the implants. Implants of commercially pure titanium (grade IV) with a surface treated by double acid attack (nitric, hydrofluoric and sulfuric acids), with a diameter of 1.5mm and height of 3.5mm (Neodent, JJGC dental materials industry and trade S.A., Curitiba, PR, Brazil) were installed in each tibial of the rats. The tissues were sutured in planes using absorbable yarn (Poligalactin 910, Vycril 4.0, Ethicon, Brazil). In the immediate postoperative period, each animal received a single intramuscular dose of 0.2ml Penicillin G-benzathine (Zoetis, Fort Dodge Health Animal, Campinas, SP, Brazil).

2.4 Application of fluorochromes

For the analysis of confocal microscopy, were injected the fluorochromes in 6 animals of each group intramuscularly at the dosage of 20mg/kg. The application of injection of calcein fluorochrome (Sigma Aldrich Brazil Ltda, São Paulo, SP, Brazil) was at 14 days after the implant installation and Alizarin red fluorochrome (Sigma Aldrich Brazil Ltda, São Paulo, SP, Brazil) at 42 days (Faverani et al. 2018; Ramalho-Ferreira et al. 2017).

2.5 Euthanasia and obtaining samples

The animals were anesthetized with a lethal dose of sodium thiopental 1g (Thiopentax, Cristália Chemicals and Pharmaceuticals Ltda, Itapira, SP, Brazil). Euthanasia of 18 animals (n=6/group) was performed 42 days after implant installation. One of the tibiae was submitted to the biomechanical test (N= 6 tibiae/group) and the remnant bone was collected and stored in liquid nitrogen for real-time PCR analysis, the other tibia of the animal was removed and fixed in buffered 10% formalin solution (Analytical Reagents, Hospital Dynamics, Brazil) for the immunohistochemical analyzes. The other 18 animals were sacrificed after 60 days of implant placement, the tibiae were removed and fixed for 48 hours, bathed in running water for 24 hours and stored in alcohol 70 for analysis by computerized microtomography and by confocal microscopy.

2.6 Biomechanical test

A digital implant wrench (Conexão, Prosthesis Systems, Brazil) was adapted to the implant and a digital torque meter (Instrutherm, Brazil) was adapted over it. A counter-clockwise movement was applied by increasing the reverse rotation torque to the implant within the bone tissue until withdraw from the bone (Ramalho-Ferreira et al. 2015). The torque meter then recorded the peak torque in Newton centimeters (N.cm).

2.7 Molecular analysis (PCR)

Total RNA of the remnant bone was extracted with Trizol reagent (Promega Corporation, Madison, WI, USA) and converted into cDNA (Life kit; Life Technologies, Invitrogen, Carlsbad, CA, USA). Real-time PCR was performed with the StepOnePlus

(Applied Biosystems, Waltham, MA USA) using SYBR Green (Applied Biosystems). Beta-actin and beta-2 microglobulin (Life Biotechnologies, Invitrogen, Carlsbad, CA, USA) were used for normalization of OPG (osteoprotegerin), RANKL (receptor activator of nuclear factor-kappaB ligand), OCN (osteocalcin) and ALP (alkaline phosphatase) expression using the delta CT method. Primer sequences have been reported recently. Data represent quadruplicates. (Yogui et al. 2018)

2.8 Morphometric Analysis

The samples were fixed for 48 hours and bathed in running water for 24 hours. Subsequently, decalcification of the tibiae in EDTA (10%) was carried out for five weeks, followed by dehydration with a sequence of alcohols, then diaphanization with xylene and included in paraffin. From the parts in paraffin, slices of 6µm thick were obtained and mounted on microscope slides.

After the processing of the slides with hematoxylin and eosin (HE), the images were captured by camera (Leica DFC 300 FX, Leica microsystem, Switzerland) attached to a light microscope (Leica Aristoplan Microsystem-Leitz, Germany), in 12.5x and 40x objective.

2.9 Immunolabeling Analysis

The immunohistochemical procedure started by deparaffinization and rehydration of slices. Endogenous peroxidase activity was inhibited with hydrogen peroxide and, the slides underwent antigenic recovery with phosphate citrate buffer (pH 6.0) in moist heat. Endogenous biotin was blocked with skimmed milk. As a method of blocking non-specific immunolabeling, the primary antibody was prepared in phosphate buffer and bovine albumin solution.

The primary polyclonal antibodies produced in goats were RUNX2 (Runt-related transcription factor 2) (Santa Cruz Biotechnology, Dallas, Texas, EUA - SC8566), OPN (Osteopontin) (SC10593), OCN (Osteocalcin) (SC18319) and ALP (Alkaline Phosphatase) (SC23430). The secondary antibody used for the biotinylated ant goat antibody, produced in rabbits (Pierce Biotechnology). The reaction signal was amplified by incubation in avidin and biotin (ABC standard kit, Vector Laboratories) and the reaction was developed using Diaminobenzidine (Dako laboratories). The counterstaining with Harris hematoxylin was

performed. The slide images were obtained by optical microscope (Nikon, Eclipse 80i, Shinagawa, Tokyo, Japan), 25x objective.

The expression of these proteins was evaluated by qualitative ordinal analysis by assigning different scores according to the number of cells and area of extracellular matrix immunolabeling. The analyzer was submitted to the Kappa test, with above 0.8 index obtained, showing that the observed scores were consistent (Manrique et al 2015; Palin et al 2018; Pedrosa et al 2009). The scores used were 1 (light labeling), 2 (moderate labeling) and 3 (intense labeling).

2.9.1 Microtomographic analysis – Micro-CT

For the micro-CT analysis, the samples were scanned by the SkyScan microtomograph (SkyScan 1272 Bruker MicroCT, Aatselaar, Belgium, 2003) using 6 μ m slices (90Kv and 111 μ A), with Al 0.5 + Cu 0.038 filters and a rotation step of 0.5mm, which were scanned in 360 degrees, at acquisition time of approximately 1 hour and 32 minutes. The obtained images were processed by the software NRecon (SkyScan, 2011; Version 1.6.6.0) that made the reconstruction 2D from the tomographic cuts using Smoothing 1, Ring Artifact Correction 8 and Beam Hardening Correction 24%. In the Data Viewer software (SkyScan, Version 1.4.4 64-bit) the reconstructed images were adequate in standard positioning for all the samples, being able to be observed in three planes (transversal, longitudinal and sagittal). Then, the software CTAnalyser - CTAn (2003-11SkyScan, 2012 Bruker MicroCT Version 1.12.4.0) was used, evaluate the region between the 3rd and 5th implants in 100 slices that were counted from their most central portion (Glosel et al., 2010). From the location of the cancellous bone structure, the software performed the morphometric calculation applied to the ROI through the parameters of bone volume percentage (BV/TV), trabecular thickness (Tb.Th), trabecular number (Tb.N) and trabecular separation (Tb.Sp) (Bouxsein et al., 2010).

2.10 Confocal Microscopy

For confocal microscopy analysis, the biopsies went through the dehydration step from the increasing sequence of alcohols. The samples were immersed in a mixture of absolute alcohol and Techno Vit® light-curing resin (Germany, Heraeus Kulzer GmbH Division Technik Philipp-Reis-Str. 8/13 D-61273 Wehrheim) in different concentrations, until the use of resin only. The samples were included in the Technovit resin and photopolymerized. The

cuts were performed in the mesio-distal plane using the Exakt cutting system (Exakt Cutting System, Apparatebau, Gmbh, Hamburg, Germany) until obtaining a section of 80µm thick, mounted on slides and stabilized with mineral oil. Longitudinal sections of the bone-implant interface corresponding to the third -fourth implant thread was captured using a Leica CTR 4000 CS SPE camera (Leica Microsystems, Heidelberg, Germany) in 10x objective. The confocal microscopy images were reconstructed, generating photomicrographs of peri-implant bone incorporated by calcein and Alizarin red fluorochromes separately (old and new bone). The images were transported to the image J program (ImageJ® 2.1.4.7.i1, Ontario, ON, Canada), and from this, the area of precipitation of the fluorochromes in the bone thread was calculated (Dempster et al. 2012), the bone turnover was evaluated by the mineral apposition rate and also the histometric analysis of the linear extension of bone and implant contact (BIC) and the neoformed bone area (NBA) in the third to fifth implant thread region was performed according Faverani et al. 2018 and Ramalho-Ferreira et al. 2015.

2.11 Statistical Analysis

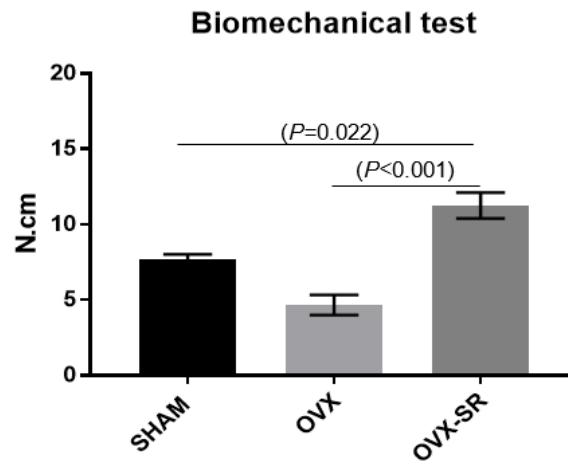
The data were tabulated and the statistics were performed in the Sigma Plot 12.0 program. Oneway Anova test was performed for comparisons between groups. The normality test was the Shapiro-Wilk test and when necessary for comparison between groups, the Tukey test was used. The level of significance was 5% ($P<0.05$).

3. Results

3.1 Biomechanical Analysis

In biomechanical analysis, the lowest reverse torque value was in the OVX. The group treated with strontium ranelate had the highest value when compared to OVX (11.25, ± 1.71 N.cm versus 4.67, ± 1.15 N.cm, $P<0.001$), such as SHAM (11.25 N.cm versus 7.67, ± 0.57 N.cm, $P=0.022$) (Graphic 1).

Graphic 1 - Biomechanical test. 42 days after implant surgery. SD: Mean with SEM.



Source: Authors.

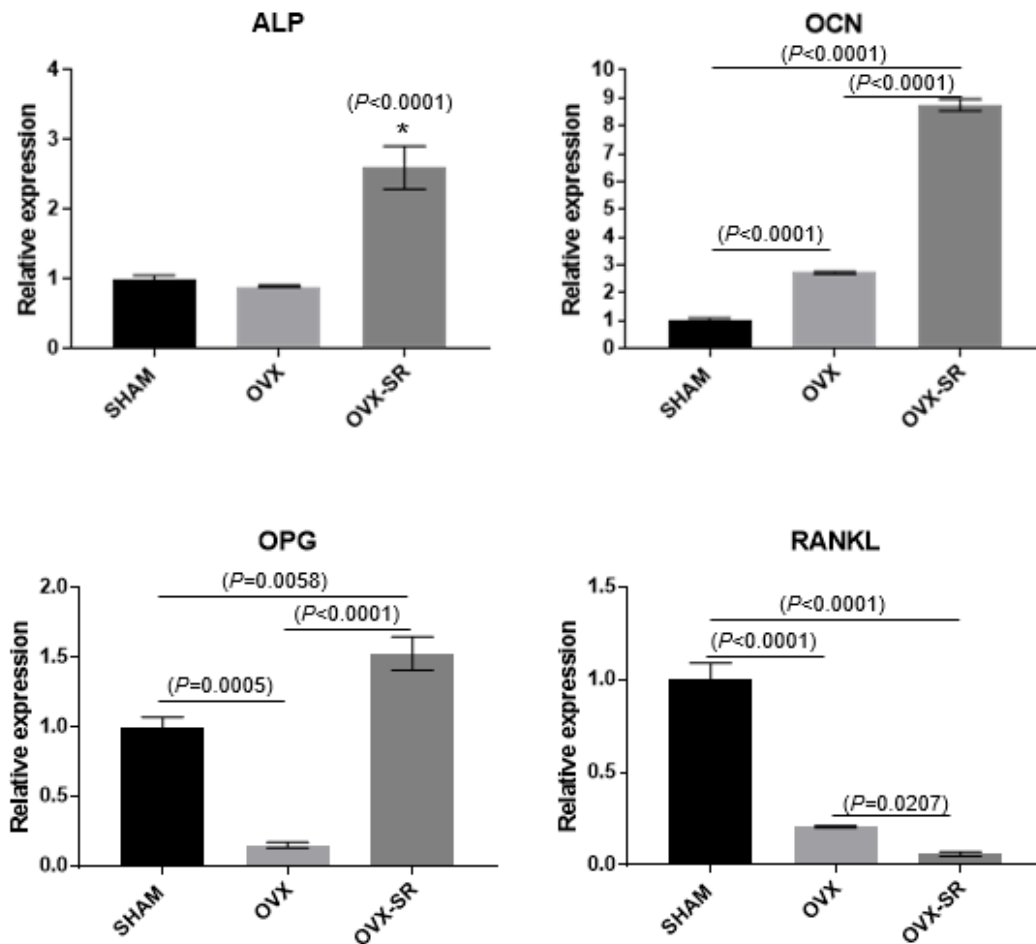
3.2 Molecular Analysis (PCR)

Relative gene expression for ALP, the enzyme that induces phosphate precipitation over bone matrix, was significantly higher in OVX-SR compared to the other groups ($P<0.0001$).

For non-collagen protein OCN, which signals bone mineralization, presented higher values of relative gene expression in OVX-SR compared to SHAM and OVX groups ($P<0.0001$).

Regarding OPG and RANKL proteins, the OVX-SR group presented the highest expression for OPG and the lowest expression for RANKL among the studied groups (Graphic 2).

Graphic 2 - Relative gene expression for ALP, OCN, OPG and RANKL. 42 days after implant surgery.

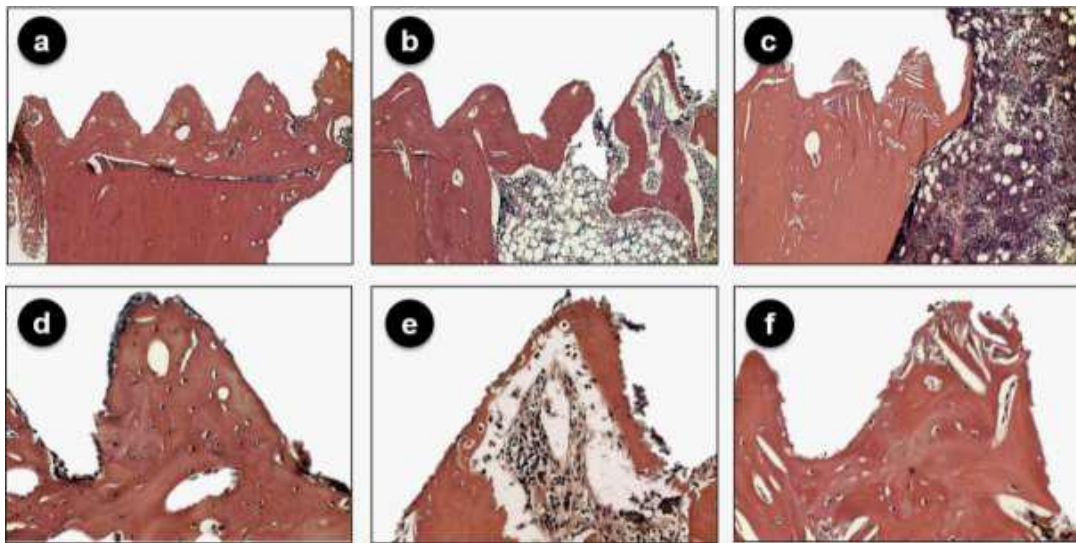


Source: Authors.

3.3 Morphometric Analysis

Histological analysis shows that the peri-implant repair in the SHAM showed a greater degree of corticalization in the osseointegration area in all corresponding spaces around the implants, with formation of mature bone tissue. In the OVX, there was formation of new bone with corticalization only in the first implants thread, and in the more superficial portions. In the medullary portion, small area of bone formation was observed in contrast to the large amount of adipose tissue observed in this region. In the OVX-Sr, an improvement in the maturation of peri-implant bone tissue was observed with histological images very close to those of the SHAM.

Figure 1 - Histological slides of the peri-implant bone in the SHAM (a, d), OVX (b, e) and OVX-Sr (c, f) groups. Evaluation period is 42 days after implant installation. HE staining. Original magnification 12.5x (a-c) and 40x (d-f).



Source: Authors.

3.4 Immunolabeling Analysis

Immunolabels were evaluated in the region of bone tissue formed next to the implants, to characterize the different cell stages of the osteoblastic lineage, was observed the presence of the RUNX2, positive in pre-osteoblasts and osteoblasts. The ALP labeling the activity of alkaline phosphate precipitation on the organic matrix of type I collagen. OPN, positive for cells of the osteoblastic lineage and shows the calcium precipitation activity on the organic matrix based on type I collagen, and OCN, labels mature osteoblasts at the end of the mineralization phase of calcium on the organic matrix of collagen.

RUNX2 was positively showed in all experimental groups. SHAM and OVX-Sr groups showed moderate labeling. OVX presented an intense labeling, however it occurred in the non-mineralized tissue.

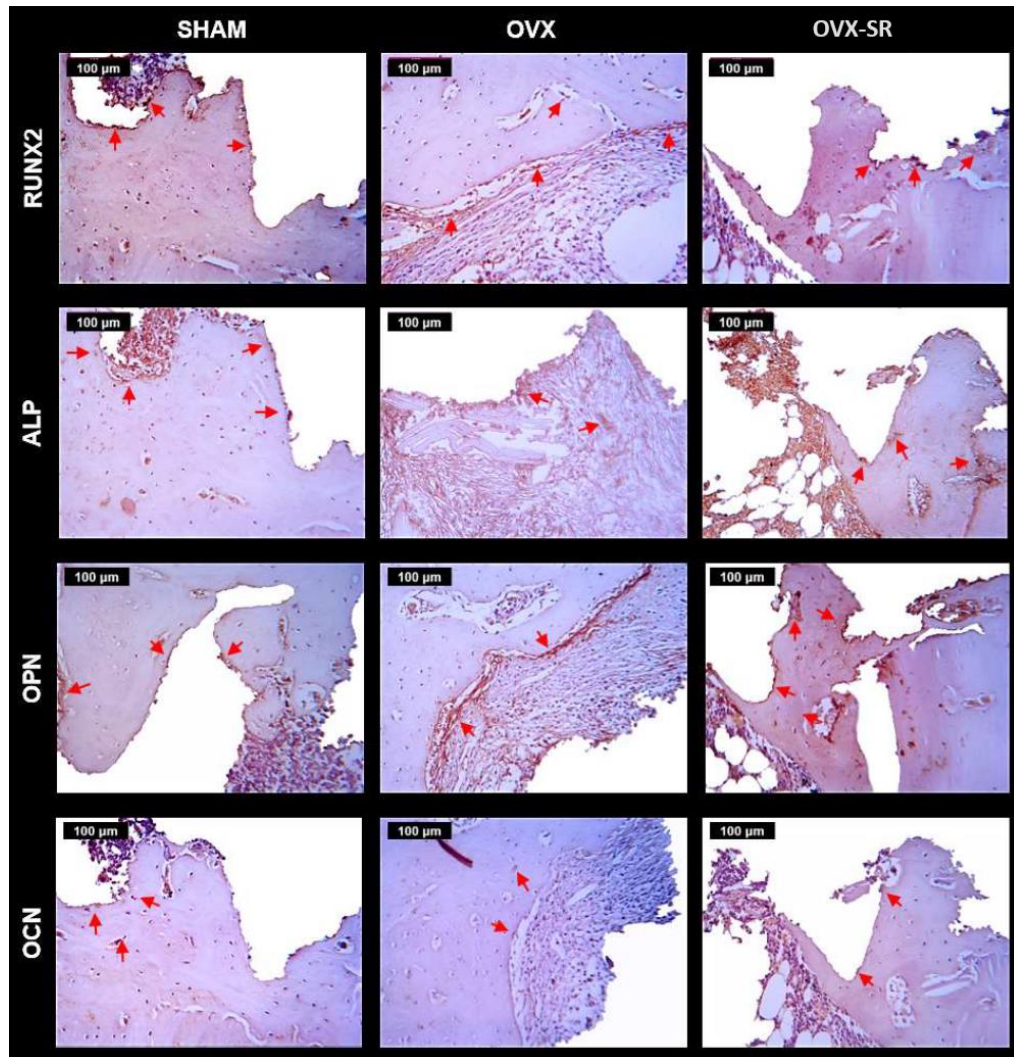
Intense labeling for ALP was observed in the SHAM. In the OVX, a light labeling was observed. After treatment with Ran-Sr, moderate staining was observed for ALP in osteoblasts present in the bone tissue.

In SHAM and OVX-Sr, moderate labeling for OPN was showed, especially for endosteal cells. In the OVX, discrete labeling was observed in connective tissue.

In the SHAM, the OCN showed moderate labeling in osteocytes in the bone tissue formed around to the implants. In OVX, light labeling was observed for OCN in cells similar

to osteoblasts without mineralization characteristics. The OVX-Sr presented bone tissue around the implant with a light labeling for OCN in the osteocytes of this region.

Figure 2 - Immunolabeling of RUNX2, ALP, OPN and OCN proteins for the SHAM, OVX and OVX-SR groups. Original magnification 20x; Red Arrows = immunolabeling.

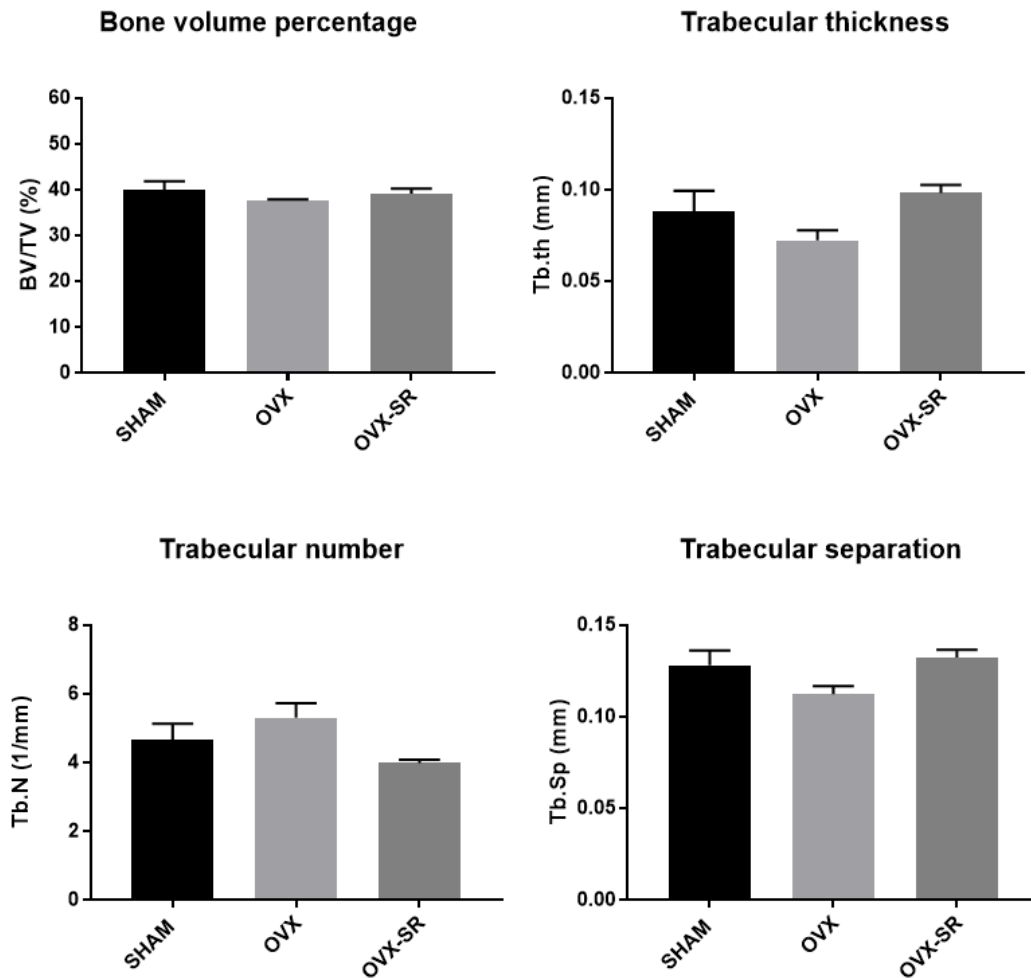


Source: Authors.

3.5 Microtomographic analysis

There were no significant differences between groups for the parameters evaluated in microtomography (Graphic 3).

Graphic 3 - Microtomographic analysis of BV/TV, Tb.Th, Tb.N and Tb.Sp. 60 days after implant surgery. SD: Mean with SEM.



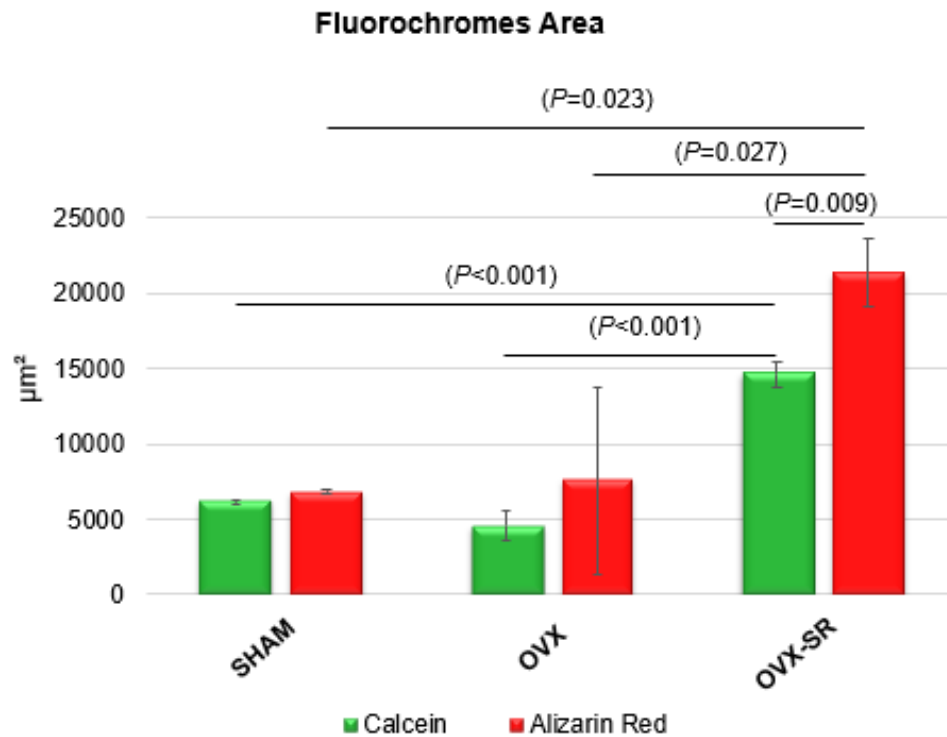
Source: Authors.

3.6 Confocal microscopy

Bone Dynamics

In the intra-group evaluation of the fluorochromes area, the highest bone turnover in bone thread was evident in the OVX-SR group, represented by the higher precipitation of flourochromes, mainly due to the greater presence of Alizarina in relation to calcein ($P=0.009$). In the intergroup evaluation, the OVX-SR group showed higher calcein precipitation than SHAM and OVX ($P<0.001$), as well as alizarin precipitation ($P<0.05$) (Graphic 4).

Graphic 4 - Calcein and Alizarin red Fluorochromes area. 60 days after implant surgery Calcein injected at 14 days (old bone) and Alizarin red at 42 days after implant placement (new bone). SD: Mean with SEM.

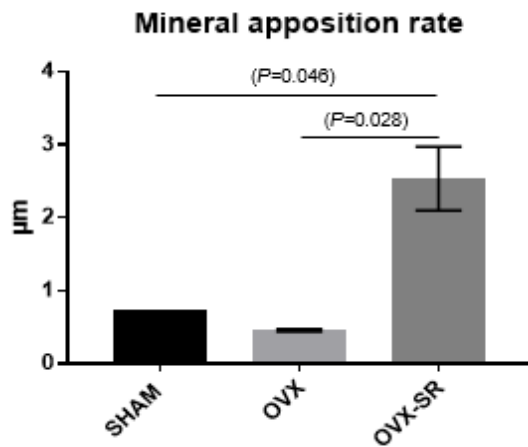


Source: Authors.

Mineral apposition rate

Regarding the rate of mineral apposition per day of bone around the implant, the highest values were in OVX-SR (2.54 µm/day, $P < 0.05$), followed by SHAM (0.75 µm/day) and OVX (0.45 µm/day) (Graphic 5).

Graphic 5 - Mineral apposition rate per day. 60 days after implant surgery. SD: Mean with SEM.

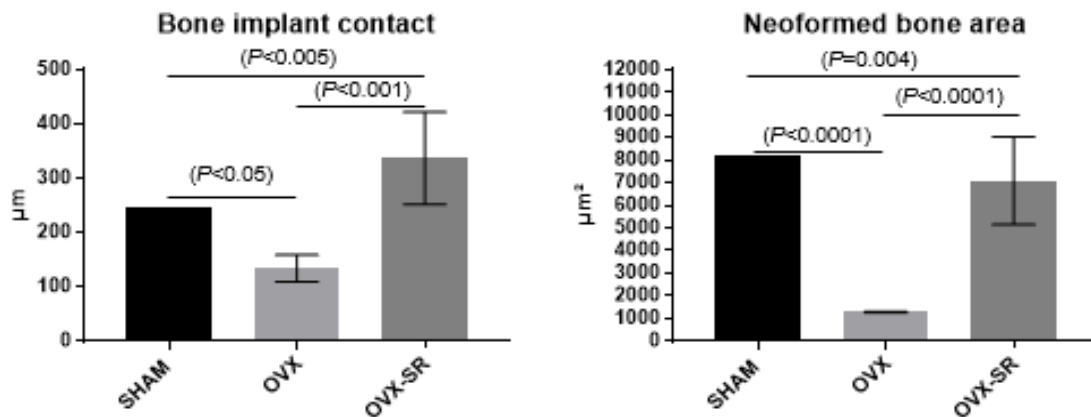


Source: Authors.

Histometric analysis – BIC and NBA

In the BIC, the OVX-Sr showed the largest contact area between the newly formed bone tissue and the implant surface (337.12µm), successive to the SHAM (245.6µm), and the OVX had the lowest linear extent of bone/implant contact (134.07µm). All groups had a statistical difference when compared ($p < 0.05$). In the results obtained by the histometric analysis for NBA, the SHAM had the largest neoformed bone area (8188.19µm²), followed by the Ran-Sr (7099.41µm²), the OVX had the lowest values of newly formed bone area (1281.41µm²), as seen in the images of the peri-implant bone by confocal microscopy. There were statistical differences between all groups ($p < 0.05$) (Graphic 6).

Graphic 6 - Biomechanical test. 42 days after implant surgery. SD: Mean with SEM.



Source: Authors.

4. Discussion

SR is a bone anabolic drug, with pro-forming and anti-resorptive effects (Bonnelye et al. 2008; Marie et al. 2001). In this study, the set of results shows that systemic strontium ranelate was effective in improving several parameters related to osseointegration and evaluation of peri-implant bone tissue.

From a biomechanical point of view, the counter-torque showed that SR improves the biomechanical characteristics of the reparative bone tissue. These data are corroborated by analyses of static and dynamic fluorochromic histometry. In this last analysis, the mineral apposition rate data confirm the anabolic effect of SR, where an important daily mineral apposition rate was observed.

These findings are corroborated by PCR and immunohistochemistry analyses. The evaluated genes show that mineral precipitation is increased with SR treatment, showing significant increase for both ALP and OC. Regarding the responses of resorption and bone formation, the genes for OPG and RANKL show antagonistic behaviour, OPG, a marker of bone formation, was shown to be increased in the RE group and in compensation, RANKL, a marker of resorption was shown to be significantly decreased in this same group. Immunolabels related to bone formation and extracellular matrix proteins showed similar behavior for the SHAM and OVX-Sr groups, which once again shows the favorable responses to bone metabolism observed for this medication.

At the cellular/tissue level, it is known the mechanism of action of SR in osteoblasts, with the induced proliferation of preosteoblasts, increases the activity of osteoblasts leads to a greater expression of proteins related to the bone matrix (Bonnelye et al. 2008), these data were also observed in this study by increasing the expression of markers such as alkaline phosphatase and osteocalcin. In a study in patients with osteoporosis treated with SR (Marie PJ, 2005) an increase in serum levels of alkaline phosphatase was observed from the third month of treatment, and was maintained after 3 years of treatment.

On the other hand, strontium inhibits osteoclastic activity by the OPG/RANKL system mediated by osteoblasts with increased secretion of osteoprotegerin (OPG) and reduced expression of the nuclear factor receptor kappa-B ligand (RANKL) (Brennan et al. 2009; Cianferotti et al. 2013), results also found in this study in the analysis of immunohistochemistry of the periimplant bone and mainly by rt-PCR analysis.

In the analyses of bone dynamics and rate of mineral apposition rate the SR group was the one that presented more expressive values compared to the other groups, this can be explained because of the structural similarity of strontium with calcium, and in the same way, it is incorporated in the crystalline network of bone tissue (Blake and Fogelman, 2006; Meunier et al. 2004), besides the greater availability of this element in the bloodstream of the medicated animals. This fact can be explained because of the structural similarity of strontium with calcium, and in the same way, it is incorporated into the crystalline network of bone tissue (Blake and Fogelman, 2006; Meunier et al. 2004), in addition to the greater availability of this element in the bloodstream of medicated animals.

As for the three-dimensional evaluation, no significant changes were observed between these three groups, regarding parameters related to bone volume and characteristics of bone trabeculation. However, taking into consideration all the results, the favorable responses obtained by the SR are evident.

Strontium ranelate has restricted use in some countries due to reports of increased incidence of venous thromboembolism, myocardial infarction (Stevenson et al. 2007; European Medicines Agency) and cardiac risk with its use (Abrahamsen et al. 2014; Cooper et al. 2014). However, Yu et al. 2015, shows that one-half of patients with osteoporosis treated with strontium ranelate had cardiovascular risk factors prior to initiation of treatment. Martín-Merino et al. 2018, shows that osteoporotic patients treated with different drugs in Spain and the United Kingdom, they report that there is no data to support an increased risk of venous thromboembolism associated with strontium ranelate compared to other drugs.

The findings of this study corroborate the systematic review study in animals that evaluated the relationship of SR with osseointegration (Scardueli et al. 2018) and certainly SR has a potent anabolic effect on bone tissue, which leads to increased osseointegration/stabilization of implants. However, this drug is being used only for cases of severe osteoporosis (Reginster et al. 2015) (being withdrawn from the market) due to its cardiovascular adverse effects in patients who have used SR (Confavreux et al. 2012; Reginster et al. 2015).

Despite the promising results, it is important to evaluate how much the positive response on bone metabolism persists over time, and most important, to evaluate possible adverse responses that may occur as a result of the use of this medication.

5. Final Considerations

Even with the limitations of this study, it can be concluded that SR presents an important anabolic effect on periimplant bone tissue in rats with estrogen deficiency, promoting improvement in bone repair after the installation of implants. However, further studies are needed to define the real mechanisms of action of this compound on cardiovascular tissue and also to investigate whether these side effects are also observed in biomaterials containing strontium used as bone substitutes.

Acknowledgements

This study was financially supported by National Council for Scientific and Technological Development – CNPq – fellowship Roberta Okamoto (306389/2017-7) and São Paulo Research Foundation – FAPESP (2015/14688-0, 2015/13712-4 and 2016/03790-0). The authors would also thank Neodent for the implants used in this research.

References

Abrahamsen, B., Grove, E. L., & Vestergaard, P. (2014). Nationwide registry-based analysis of cardiovascular risk factors and adverse outcomes in patients treated with strontium ranelate. *Osteoporosis international*, 25(2), 757–762. <https://doi.org/10.1007/s00198-013-2469-4>

Bain, S. D., Jerome, C., Shen, V., Dupin-Roger, I., & Ammann, P. (2009). Strontium ranelate improves bone strength in ovariectomized rat by positively influencing bone resistance determinants. *Osteoporosis international*, 20(8), 1417–1428. <https://doi.org/10.1007/s00198-008-0815-8>.

Beattie, J. R., Sophocleous, A., Caraher, M. C., O'Driscoll, O., Cummins, N. M., Bell, S., Towler, M., Rahimnejad Yazdi, A., Ralston, S. H., & Idris, A. I. (2019). Raman spectroscopy as a predictive tool for monitoring osteoporosis therapy in a rat model of postmenopausal osteoporosis. *Journal of materials science. Materials in medicine*, 30(2), 25. <https://doi.org/10.1007/s10856-019-6226-x>

Blake, G. M., & Fogelman, I. (2006). Theoretical model for the interpretation of BMD scans in patients stopping strontium ranelate treatment. *Journal of bone and mineral research*, 21(9), 1417–1424. <https://doi.org/10.1359/jbmr.060616>

Brennan, T. C., Rybchyn, M. S., Green, W., Atwa, S., Conigrave, A. D., & Mason, R. S. (2009). Osteoblasts play key roles in the mechanisms of action of strontium ranelate. *British journal of pharmacology*, 157(7), 1291–1300. <https://doi.org/10.1111/j.1476-5381.2009.00305.x>

Bonnelye, E., Chabadel, A., Saltel, F., & Jurdic, P. (2008). Dual effect of strontium ranelate: stimulation of osteoblast differentiation and inhibition of osteoclast formation and resorption in vitro. *Bone*, 42(1), 129–138. <https://doi.org/10.1016/j.bone.2007.08.043>

Bouxsein, M. L., Boyd, S. K., Christiansen, B. A., Guldberg, R. E., Jepsen, K. J. & Müller, R. (2010) Guidelines for assessment of bone microstructure in rodents using micro-computed tomography. *J Bone Miner Res.* 25(7):1468-86. <https://doi.org/10.1002/jbmr.141>.

Cianferotti, L., D'Asta, F., & Brandi, M. L. (2013). A review on strontium ranelate long-term antifracture efficacy in the treatment of postmenopausal osteoporosis. *Therapeutic advances in musculoskeletal disease*, 5(3), 127–139. <https://doi.org/10.1177/1759720X13483187>

Cooper, C., Fox, K. M., & Borer, J. S. (2014). Ischaemic cardiac events and use of strontium ranelate in postmenopausal osteoporosis: a nested case-control study in the

CPRD. *Osteoporosis international*, 25(2), 737–745. <https://doi.org/10.1007/s00198-013-2582-4>

Compston, J. E., McClung, M. R., & Leslie, W. D. (2019). Osteoporosis. *Lancet (London, England)*, 393(10169), 364–376. [https://doi.org/10.1016/S0140-6736\(18\)32112-3](https://doi.org/10.1016/S0140-6736(18)32112-3)

Confavreux, C. B., Canoui-Poitaine, F., Schott, A. M., Ambrosi, V., Tainturier, V., & Chapurlat, R. D. (2012). Persistence at 1 year of oral antiosteoporotic drugs: a prospective study in a comprehensive health insurance database. *European journal of endocrinology*, 166(4), 735–741. <https://doi.org/10.1530/EJE-11-0959>

Cosman, F., de Beur, S. J., LeBoff, M. S., Lewiecki, E. M., Tanner, B., Randall, S., Lindsay, R., & National Osteoporosis Foundation (2014). Clinician's Guide to Prevention and Treatment of Osteoporosis. *Osteoporosis international*, 25(10), 2359–2381. <https://doi.org/10.1007/s00198-014-2794-2>

Dempster, D. W., Compston, J. E., Drezner, M. K., Glorieux, F. H., Kanis, J. A. & Malluche, H. (2013) Standardized nomenclature, symbols, and units for bone histomorphometry: a 2012 update of the report of the ASBMR Histomorphometry Nomenclature Committee. *J Bone Miner Res.* 28(1):2-17.

European Medicines Agency PSUR assessment report: Strontium ranelate. 2013. Retrieved from http://www.ema.europa.eu/docs/en_GB/document_library/EPAR__Assessment_Report_-_Variation/human/000560/WC500147168.pdf

Faverani, L. P., Polo, T., Ramalho-Ferreira, G., Momesso, G., Hassumi, J. S., Rossi, A. C., Freire, A. R., Prado, F. B., Luvizuto, E. R., Gruber, R., & Okamoto, R. (2018). Raloxifene but not alendronate can compensate the impaired osseointegration in osteoporotic rats. *Clinical oral investigations*, 22(1), 255–265. <https://doi.org/10.1007/s00784-017-2106-2>

Glösel, B., Kuchler, U., Watzek, G., & Gruber, R. (2010). Review of dental implant rat research models simulating osteoporosis or diabetes. *The International journal of oral & maxillofacial implants*, 25(3), 516–524.

Grynepas, M. D., & Marie, P. J. (1990). Effects of low doses of strontium on bone quality and quantity in rats. *Bone*, 11(5), 313–319. [https://doi.org/10.1016/8756-3282\(90\)90086-e](https://doi.org/10.1016/8756-3282(90)90086-e)

Hamdy N. A. (2009). Strontium ranelate improves bone microarchitecture in osteoporosis. *Rheumatology (Oxford, England)*, 48 Suppl 4, iv9–iv13. <https://doi.org/10.1093/rheumatology/kep274>

Hurtel-Lemaire, A. S., Mentaverri, R., Caudrillier, A., Cournarie, F., Wattel, A., Kamel, S., Terwilliger, E. F., Brown, E. M., & Brazier, M. (2009). The calcium-sensing receptor is involved in strontium ranelate-induced osteoclast apoptosis. New insights into the associated signaling pathways. *The Journal of biological chemistry*, 284(1), 575–584. <https://doi.org/10.1074/jbc.M801668200>.

International Osteoporosis Foundation. Retrieved from <https://www.iofbonehealth.org/>

Kilkenny, C., Browne, W. J., Cuthill, I. C., Emerson, M. & Altman, D. G. (2010) Improving bioscience reporting: the ARRIVE guidelines for reporting animal research. *PLoS Biol.* 29;8(6):e1000412. <https://doi.org/10.1371/journal.pbio.1000412>.

Maimoun, L., Brennan, T. C., Badoud, I., Dubois-Ferriere, V., Rizzoli, R., & Ammann, P. (2010). Strontium ranelate improves implant osseointegration. *Bone*, 46(5), 1436–1441. <https://doi.org/10.1016/j.bone.2010.01.379>

Manrique, N., Pereira, C. C., Luvizuto, E. R., Sánchez, M. del P., Okamoto, T., Okamoto, R., Sumida, D. H. & Antoniali, C. (2015) Hypertension modifies OPG, RANK, and RANKL expression. during the dental socket bone healing process in spontaneously hypertensive rats. *Clin Oral Investig.* 19(6):1319-27. <https://doi.org/10.1007/s00784-014-1369-0>.

Marie, P. J., Ammann, P., Boivin, G., & Rey, C. (2001). Mechanisms of action and therapeutic potential of strontium in bone. *Calcified tissue international*, 69(3), 121–129. <https://doi.org/10.1007/s002230010055>

Marie P. J. (2005). Strontium as therapy for osteoporosis. *Current opinion in pharmacology*, 5(6), 633–636. <https://doi.org/10.1016/j.coph.2005.05.005>

Martín-Merino, E., Petersen, I., Hawley, S., Álvarez-Gutierrez, A., Khalid, S., Llorente-García, A., Delmestri, A., Javaid, M. K., Van Staa, T. P., Judge, A., Cooper, C., & Prieto-Alhambra, D. (2018). Risk of venous thromboembolism among users of different anti-osteoporosis drugs: a population-based cohort analysis including over 200,000 participants from Spain and the UK. *Osteoporosis international*, 29(2), 467–478. <https://doi.org/10.1007/s00198-017-4308-5>

Meunier, P. J., Roux, C., Seeman, E., Ortolani, S., Badurski, J. E., Spector, T. D., Cannata, J., Balogh, A., Lemmel, E. M., Pors-Nielsen, S., Rizzoli, R., Genant, H. K., & Reginster, J. Y. (2004). The effects of strontium ranelate on the risk of vertebral fracture in women with postmenopausal osteoporosis. *The New England journal of medicine*, 350(5), 459–468. <https://doi.org/10.1056/NEJMoa022436>.

Palin, L. P., Polo, T. O. B., Batista, F. R. S., Gomes-Ferreira, P. H. S., Garcia-Junior, I. R., Rossi, A. C., Freire, A., Faverani, L. P., Sumida, D. H. & Okamoto, R. (2018) Daily melatonin administration improves osseointegration in pinealectomized rats. *J Appl Oral Sci.* 10;26: e20170470. <https://doi.org/10.1590/1678-7757-2017-0470>.

Pedrosa, W. F. Jr, Okamoto, R., Faria, P. E., Arnez, M. F., Xavier, S. P. & Salata, L. A. (2009) Immunohistochemical, tomographic and histological study on onlay bone graft remodeling. Part II: calvarial bone. *Clin Oral Implants Res.* 20(11):1254-64. <https://doi.org/10.1111/j.1600-0501.2009.01747.x>.

Pilmane, M., Salma-Ancane, K., Loca, D., Locs, J., & Berzina-Cimdina, L. (2017). Strontium and strontium ranelate: Historical review of some of their functions. *Materials science & engineering. C, Materials for biological applications*, 78, 1222–1230. <https://doi.org/10.1016/j.msec.2017.05.042>

Ramalho-Ferreira, G., Faverani, L. P., Prado, F. B., Garcia, I. R., Jr, & Okamoto, R. (2015). Raloxifene enhances peri-implant bone healing in osteoporotic rats. *International journal of oral and maxillofacial surgery*, 44(6), 798–805. <https://doi.org/10.1016/j.ijom.2015.02.018>

Ramalho-Ferreira, G., Faverani, L. P., Momesso, G., Luvizuto, E. R., de Oliveira Puttini, I., & Okamoto, R. (2017). Effect of antiresorptive drugs in the alveolar bone healing. A histometric and immunohistochemical study in ovariectomized rats. *Clinical oral investigations*, 21(5), 1485–1494. <https://doi.org/10.1007/s00784-016-1909-x>

Reginster, J. Y., Sarlet, N., Lejeune, E., & Leonori, L. (2005). Strontium ranelate: a new treatment for postmenopausal osteoporosis with a dual mode of action. *Current osteoporosis reports*, 3(1), 30–34. <https://doi.org/10.1007/s11914-005-0025-7>

Reginster, J. Y., Brandi, M. L., Cannata-Andía, J., Cooper, C., Cortet, B., Feron, J. M., Genant, H., Palacios, S., Ringe, J. D., & Rizzoli, R. (2015). The position of strontium ranelate in today's management of osteoporosis. *Osteoporosis international*, 26(6), 1667–1671. <https://doi.org/10.1007/s00198-015-3109-y>

Scardueli, C. R., Bizelli-Silveira, C., Marcantonio, R., Marcantonio, E., Jr, Stavropoulos, A., & Spin-Neto, R. (2018). Systemic administration of strontium ranelate to enhance the osseointegration of implants: systematic review of animal studies. *International journal of implant dentistry*, 4(1), 21. <https://doi.org/10.1186/s40729-018-0132-8>

Stevenson, M., Davis, S., Lloyd-Jones, M., & Beverley, C. (2007). The clinical effectiveness and cost-effectiveness of strontium ranelate for the prevention of osteoporotic fragility fractures in postmenopausal women. *Health technology assessment (Winchester, England)*, 11(4), 1–134. <https://doi.org/10.3310/hta11040>

Tarantino, U., Iolascon, G., Cianferotti, L., Masi, L., Marcucci, G., Giusti, F., Marini, F., Parri, S., Feola, M., Rao, C., Piccirilli, E., Zanetti, E. B., Cittadini, N., Alvaro, R., Moretti, A., Calafiore, D., Toro, G., Gimigliano, F., Resmini, G., & Brandi, M. L. (2017). Clinical guidelines for the prevention and treatment of osteoporosis: summary statements and recommendations from the Italian Society for Orthopaedics and Traumatology. *Journal of orthopaedics and traumatology*, 18(Suppl 1), 3–36. <https://doi.org/10.1007/s10195-017-0474-7>

Yogui, F. C., Momesso, G., Faverani, L. P., Polo, T., Ramalho-Ferreira, G., Hassumi, J. S., Rossi, A. C., Freire, A. R., Prado, F. B., & Okamoto, R. (2018). A SERM increasing the

expression of the osteoblastogenesis and mineralization-related proteins and improving quality of bone tissue in an experimental model of osteoporosis. *Journal of applied oral science : revista FOB*, 26, e20170329. <https://doi.org/10.1590/1678-7757-2017-0329>

Yu, J., Tang, J., Li, Z., Sajjan, S., O'Regan, C., Modi, A., & Sazonov, V. (2015). History of cardiovascular events and cardiovascular risk factors among patients initiating strontium ranelate for treatment of osteoporosis. *International journal of women's health*, 7, 913–918. <https://doi.org/10.2147/IJWH.S88627>

Zacchetti, G., Dayer, R., Rizzoli, R., & Ammann, P. (2014). Systemic treatment with strontium ranelate accelerates the filling of a bone defect and improves the material level properties of the healing bone. *BioMed research international*, 2014, 549785. <https://doi.org/10.1155/2014/549785>

Percentage of contribution of each author in the manuscript

Fernanda Costa Yogui – 17%

Ana Cláudia Ervolino da Silva – 14%

Letícia Pitol Palin – 9%

Juliana Zorzi Coléte – 12%

Jaqueline Suemi Hassumi – 5%

Fábio Roberto de Souza Batista – 9%

Pedro Henrique Silva Gomes-Ferreira – 9%

Naara Gabriela Monteiro – 5%

Roberta Okamoto – 17%